

OPTICAL PROPERTIES OF AMORPHOUS $\text{Se}_{80-x}\text{Te}_{20}\text{Bi}_x$ THIN FILMS

K. SHARMA^a, M. LAL^b, N. GOYAL^{a*}

^a*Department of Physics, Panjab University, Chandigarh, India-160014.*

^b*GGDSD College, Chandigarh, India-160030.*

In this paper, the effect of bismuth (Bi) content on optical properties of amorphous $\text{Se}_{80-x}\text{Te}_{20}\text{Bi}_x$ thin films has been studied. Thin films of $\text{Se}_{80-x}\text{Te}_{20}\text{Bi}_x$ glassy alloys have been prepared by thermal evaporation technique under high vacuum conditions ($\sim 10^{-4}$ Pa). The optical transmission spectra of amorphous $\text{Se}_{80-x}\text{Te}_{20}\text{Bi}_x$ ($x = 0, 2, 4, 6, 8$) thin films have been measured by a double beam UV-VIS-NIR computer controlled spectrophotometer. Swanepole method has been used to calculate the optical constants (refractive index (n), extinction coefficient (k), real dielectric constant (ϵ'), imaginary dielectric constant (ϵ'') and absorption coefficient (α) and optical band gap of amorphous $\text{Se}_{80-x}\text{Te}_{20}\text{Bi}_x$ thin films. Absorption coefficient (α) increases with incident photon energy ($h\nu$) for all the samples. The optical band gap decreases with increase of the bismuth (Bi) content. The decrease in optical band gap with increase of the Bi content has been explained on the basis of Mott and Davis Model and in terms of electronegativity difference of atoms involved.

(Received February 15, 2014; Accepted March 31, 2014)

Keywords: Thin films, Chalcogenide glasses, Defect states, Optical constants, Optical band gap

1. Introduction

Chalcogenide glasses have vast electrical, optical and technological applications, such as reversible phase change based optical recording, memory devices, optical fibers, xerography, photolithography, infrared lenses, optical amplifiers, blue laser diodes and solar cells [1–8]. Erasable recording is usually considered to be a potential replacement for conventional recording due to its high storage density and archival stability. Selenium tellurium based chalcogenides have received particular attention because of their potential for applications in electronics [9-10]. These glasses are low-phonon-energy materials and are generally transparent from the visible to infrared region. Chalcogenide glasses are known to have flexible structure, in the sense that each atom can adjust its neighboring environment to satisfy the valance requirements. Chalcogenide glasses are sensitive to the absorption of electromagnetic radiation and show a variety of photo-induced effects and various models have been put forward to explain these effects, which can be used to fabricate diffractive, wave-guide and fiber structures [11-12]. As chalcogenide glasses have poor thermo-mechanical properties, in order to enlarge their domain of applications, it is necessary to increase their softening temperature and mechanical strength. The interest in these materials arises particularly due to their ease of fabrication in the form of bulk and thin films.

In pure state Se has several disadvantages because of its short life time and low sensitivity. To overcome these difficulties, certain additives are used, e.g. Te, Sb, Bi, In, Ge, etc and binary and ternary alloys are formed. Recently, it has been pointed out that Se-Te alloys have more advantages than a-Se from the technological point of view due to their greater hardness, higher crystallization temperature, higher photosensitivity and smaller ageing effects [13-17].

The effect of an impurity in an amorphous semiconductor may be widely different, depending on the conduction mechanism and the structure of material [18]. Metallic impurities such as Pb and Bi, produces a remarkable change in the electrical and optical properties of chalcogenides glasses. The conductivity type switches from p to n type on the addition of Bi.

*Corresponding author: ngoyal@pu.ac.in

In the present work Bi has been chosen as an additive element in Se-Te alloys [19-22]. The third element behaves as chemical modifier as it is reported to expand the glass forming region. The addition of third element like Bi in Se-Te binary alloy is expected to change the optical and electrical properties of host alloy. A typical chalcogenide has a relatively sharp optical absorption edge, single electrical activation energy, efficient photo excited conductivity and luminescence. The study of the optical properties of chalcogenide glasses is important for the determination of the electronic band structure as well as other optical parameters, such as optical energy gap and refractive index. The aim of present paper is to study the effect of Bi incorporation on the optical properties of Se-Te alloys. The optical transmission spectra of the amorphous thin films of $\text{Se}_{80-x}\text{Te}_{20}\text{Bi}_x$ are measured by spectrophotometer. Optical parameters like refractive index, extinction coefficient, real and imaginary dielectric constants, absorption coefficient and optical band gap have been calculated for a glassy system.

2. Experimental procedure

Glassy alloys of $\text{Se}_{80-x}\text{Te}_{20}\text{Bi}_x$ ($x = 0, 2, 4, 6, 8$) were prepared by melt-quench technique. High purity 99.999%

Bi, Se and Te granules were weighted according to the formula of $\text{Se}_{80-x}\text{Te}_{20}\text{Bi}_x$ ($x = 0, 2, 4, 6, 8$). The powder mixture was loaded into quartz ampoule and sealed under vacuum at 10^{-4} Pa. The sealed quartz ampoules was loaded in a furnace and heated to 900°C at a rate of $3\text{-}4^\circ\text{C}/\text{minute}$ for 18 hours to ensure the composition homogeneity and quenched in liquid nitrogen. The ingots were crushed, separated and grounded.

The thin films were synthesized by thermal evaporation technique under high vacuum conditions ($\sim 10^{-4}$ Pa) using a small piece of bulk alloy as a source material and glass as a substrate. The films were kept inside the deposition chamber for 24 hours to achieve the metastable equilibrium. The glassy nature of thin films was checked with the help of X-ray diffraction technique using Cu-K_α radiation. The optical transmission spectra of amorphous $\text{Se}_{80-x}\text{Te}_{20}\text{Bi}_x$ ($x = 0, 2, 4, 6, 8$) thin films have been measured by a double beam UV-VIS-NIR computer controlled spectrophotometer as a function of wavelength.

3. Result and discussion

Optical transmission (T) is a very complex function and strongly dependent on the absorption coefficient (α). The variation of transmission (T) with wavelength (λ) for amorphous $\text{Se}_{80-x}\text{Te}_{20}\text{Bi}_x$ thin films is shown in Fig. 1.

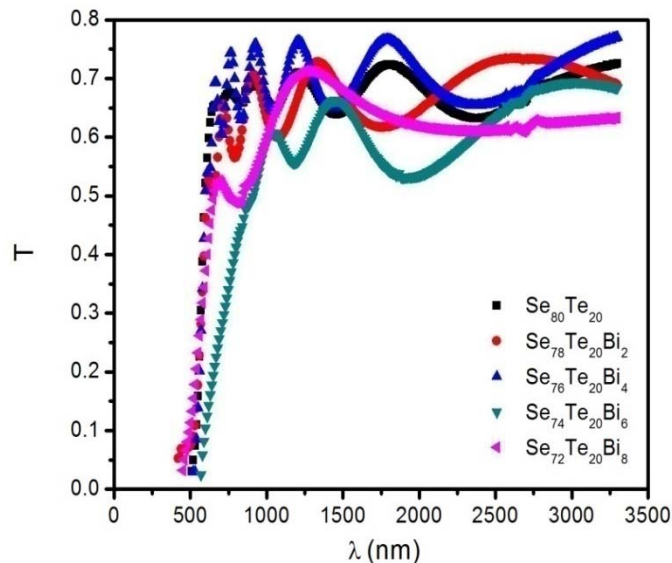


Fig. 1 Variation of transmittance (T) with wavelength (λ) for amorphous $\text{Se}_{80-x}\text{Te}_{20}\text{Bi}_x$ thin films.

According to Swanepole's method [23], which is based on Mainfacer theory [24], the envelope of the interference maxima and minima occurs in the spectrum and the presence of these maxima and minima position confirmed the optical homogeneity of the deposited film and no scattering and absorption occurs at long wavelengths. This method has been used by various workers in chalcogenide glasses [25-26].

3.1 Determination of Optical Constants

For the method proposed by Swanepole [23], the optical constants are deduced from the fringe patterns in the transmittance spectrum. In the transmittance region where the absorption coefficient ($\alpha = 0$), the refractive index n is given by

$$n = [N + (N^2 - s^2)^{1/2}]^{1/2} \quad (1)$$

where

$$N = (2s / T_m) - (s^2 + 1) / 2$$

s is the refractive index of the substrate and T_m is the envelope function of the transmittance minima.

Where ($\alpha \neq 0$), in the region of weak and medium absorption, the refractive index n is given by

$$n = [N + (N^2 - s^2)^{1/2}]^{1/2} \quad (2)$$

where

$$N = \{2s(T_M - T_m) / T_M T_m\} + (s^2 + 1) / 2$$

and T_M is the envelope function of the transmittance maxima.

In the region of strong absorption, the transmittance decreases drastically and refractive index (n) can be estimated by extrapolating the values in the other regions.

If n_1 and n_2 are the refractive indices at two adjacent maxima and minima at λ_1 and λ_2 then the thickness of the film (d) is given by

$$d = \lambda_1 \lambda_2 / 2[\lambda_1 n_2 - \lambda_2 n_1] \quad (3)$$

The extinction coefficient (k) can be calculated by relation (4)

$$k = \alpha \lambda / (4\pi) \quad (4)$$

$$= (\lambda / 4\pi d) \ln (1/x)$$

where x is the absorbance and d is the film thickness.

In the region of weak and medium absorption, absorbance (x) can be calculated from the transmission minima T_m and given in equation (5)

$$x = [E_m - \{E_m^2 - (n^2 - 1)^3 (n^2 - s^4)^{1/2}\}] / [(n - 1)^3 (n - s^2)] \quad (5)$$

$$E_m = [(8n^2 s / T_m) - (n^2 - 1) (n^2 - s^2)]$$

where

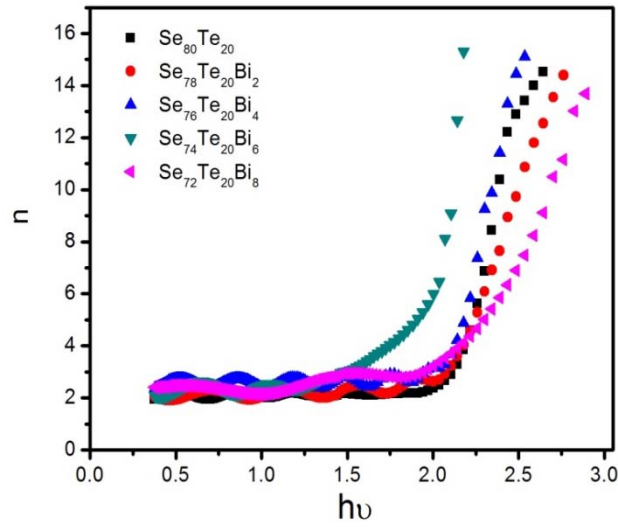


Fig 2. Variation of refractive index (n) with photon energy ($h\nu$) for amorphous $Se_{80-x}Te_{20}Bi_x$ thin films.

The calculated value of refractive index and extinction coefficient at 2100 nm are given in Table 1. The variation of refractive index and extinction coefficient with energy ($h\nu$) are shown in Figs. 2 and 3 respectively. It is observed that the value of refractive index and extinction coefficient show an overall increasing trend with the increase in photonic energy. This spectral and dopant dependence of optical constants with the photonic energy will be helpful in deciding on the suitability of this system for application in optical data storage devices.

The real and imaginary part of the dielectric constant of amorphous thin films has been calculated by the relation (6) and (7), respectively.

$$\epsilon' = n^2 - k^2 \quad (6)$$

$$\epsilon'' = 2nk \quad (7)$$

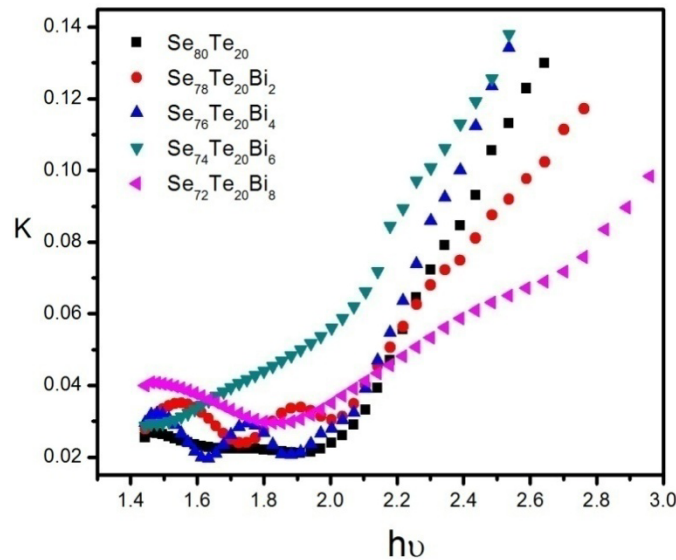


Fig 3. Variation of extinction coefficient (k) with photon energy ($h\nu$) for amorphous $Se_{80-x}Te_{20}Bi_x$ thin films.

The variation of real part and imaginary part of the dielectric constant with photonic energy is presented in Figs. 4 and 5. The calculated values of real part and imaginary part of the dielectric constant at 2100 nm are also presented in Table 1. These parameters (real part and

imaginary part of the dielectric constant) are found to increase with the increase in photon energy for $\text{Se}_{80-x}\text{Te}_{20}\text{Bi}_x$ thin films.

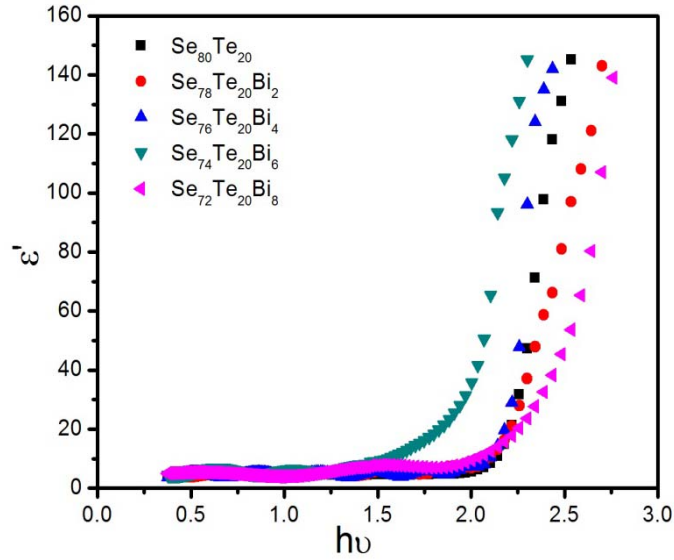


Fig 4. Variation of real dielectric constant (ϵ') with photon energy ($h\nu$) for amorphous $\text{Se}_{80-x}\text{Te}_{20}\text{Bi}_x$ thin films.

Table 1: Optical parameters for amorphous $\text{Se}_{80-x}\text{Te}_{20}\text{Bi}_x$ thin films at 2100nm.

Sample	Refractive Index (n)	Extinction Coefficient(k)	Real Dielectric Constant (ϵ')	Imaginary Dielectric Constants(ϵ'')	Absorption Coefficient (α)(m^{-1}) x 10^5	Optical Band Gap E_g (eV)
$\text{Se}_{80}\text{Te}_{20}$	2.11	0.0629	4.461	0.2672	3.884	1.75
$\text{Se}_{78}\text{Te}_{20}\text{Bi}_2$	2.14	0.0651	4.577	0.2783	3.921	1.63
$\text{Se}_{76}\text{Te}_{20}\text{Bi}_4$	2.62	0.0673	4.717	0.2926	4.728	1.52
$\text{Se}_{74}\text{Te}_{20}\text{Bi}_6$	2.72	0.0949	6.561	0.4815	5.213	1.43
$\text{Se}_{72}\text{Te}_{20}\text{Bi}_8$	2.46	0.0772	5.344	0.4073	5.122	1.25

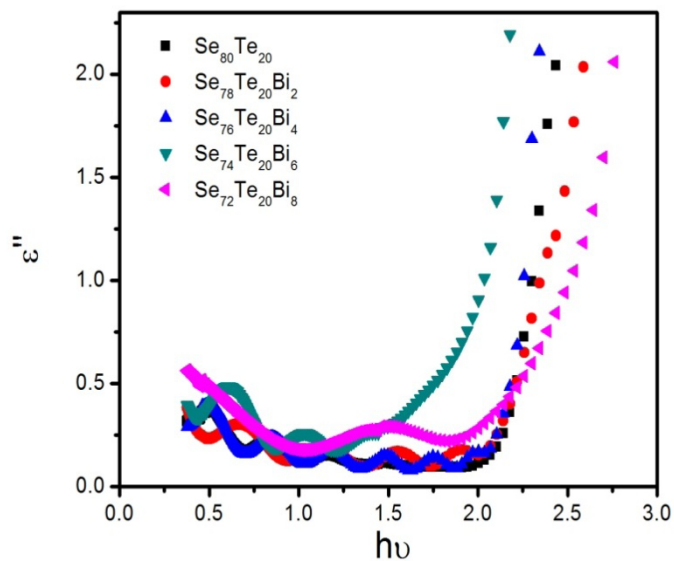


Fig 5. Variation of imaginary dielectric constant with photon energy ($h\nu$) for amorphous $\text{Se}_{80-x}\text{Te}_{20}\text{Bi}_x$ thin films.

These low dielectric constant materials will play a crucial role in the future generation of integrated circuit devices particularly for ultra-large scale integration (ULSI) and high speed IC packaging and also in demand for the next generation of interconnects to reduce the transmission delay time in integrated circuits that would allow faster intrachip and interchip communications.

3.2 Absorption coefficient

The absorption coefficient (α) of amorphous $\text{Se}_{70}\text{Te}_{30-x}\text{Sb}_x$ thin films have been calculated by using relation (9)

$$\alpha = 4\pi k / \lambda \quad (9)$$

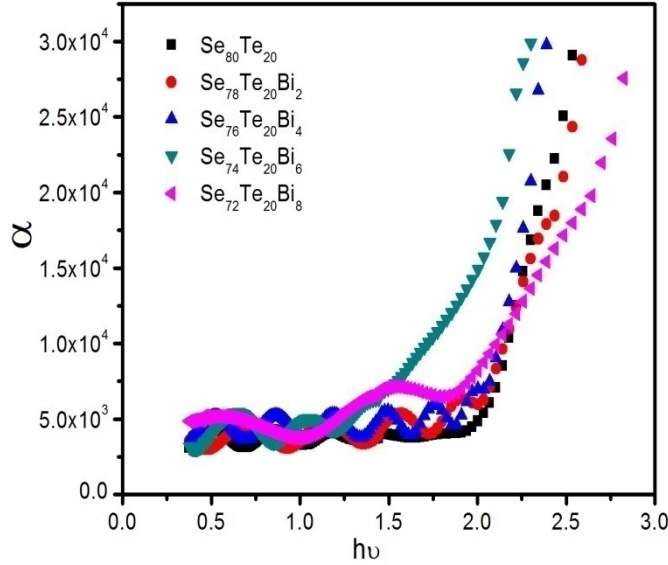


Fig 6. Variation of absorption coefficient (α) with photon energy ($h\nu$) for amorphous $\text{Se}_{80-x}\text{Te}_{20}\text{Bi}_x$ thin films.

There is an increase in the value of absorption coefficient (α) with the increase in photon energy for $\text{Se}_{80-x}\text{Te}_{20}\text{Bi}_x$ thin films and due to the large absorption coefficient these materials may be suitable for optical memory devices. At 2100 nm, the calculated values of absorption coefficient (α) for amorphous $\text{Se}_{80-x}\text{Te}_{20}\text{Bi}_x$ thin films are given in Table 1.

The optical band gap is determined from absorption coefficient data as a function of energy ($h\nu$) by using Tauc relation [27-28].

$$\alpha = A(h\nu - E_g)^n / h\nu \quad (10)$$

where A is a constant, E_g is the optical band gap of the material and the exponent n depends on the type of transition and have values $1/2$, 2 , $3/2$ and 3 corresponding to the allowed direct, allowed indirect, forbidden direct and forbidden indirect transitions, respectively. The present system of $\text{Se}_{80-x}\text{Te}_{20}\text{Bi}_x$ obeys the rule of allowed indirect transition. The values of optical band gap (E_g) is calculated by extrapolating the straight line portion of $(\alpha h\nu)^{1/n}$ vs. $h\nu$ by taking $n = 2$ as shown in Fig. 7. The calculated values of E_g for all samples are given in Table 1. It is evident from Table 1, that the optical band gap (E_g) decreases from 1.75 eV to 1.25 eV as Bi content increases from 0 to 8 at. % in the Se-Te glassy alloys. Similar trend of optical band gap with increasing Bi concentration have been observed by Suri et.al [27] while studying the optical properties of Se-Te-Bi glassy alloys. Ilyas et. al. [28] observed that the optical band gap decreases with increasing $\text{Se}_{98}\text{Bi}_2$ content in $a\text{-(Se}_{70}\text{Te}_{30})_{100-x}(\text{Se}_{98}\text{Bi}_2)_x$ thin films. Ambika et. al [29] also observed that the optical band gap decreases from 1.46 eV to 1.24 eV with variation of x from 0 to 5 at. % in $\text{Se}_{85-x}\text{Te}_{15}\text{Bi}_x$ thin films.

The decrease in optical band gap with increase of the Bi content can be explained on the basis of Mott and Davis Model [30]. According to this model, chalcogenide thin films contain a high concentration of defect states and these defects are responsible for the presence of localized

states in the band gap. The decrease in optical band gap indicates an increase in the density of defect states. The decrease in optical band gap along with the increase in the density of defect states may also be correlated with electronegativity of the elements involved. The electronegativity of Se, Te and Bi are 2.4, 2.1 and 2.0 respectively and Bi has lower electronegativity than Se. The valance band of chalcogenide glasses contains the lone pair p-orbital and addition of electropositive element (Bi) to electronegative element (Se) may raise the energy of lone pair states, which is further responsible for the broadening of the valance band inside the forbidden gap and leads to band tailing and hence band gap shrinkage.

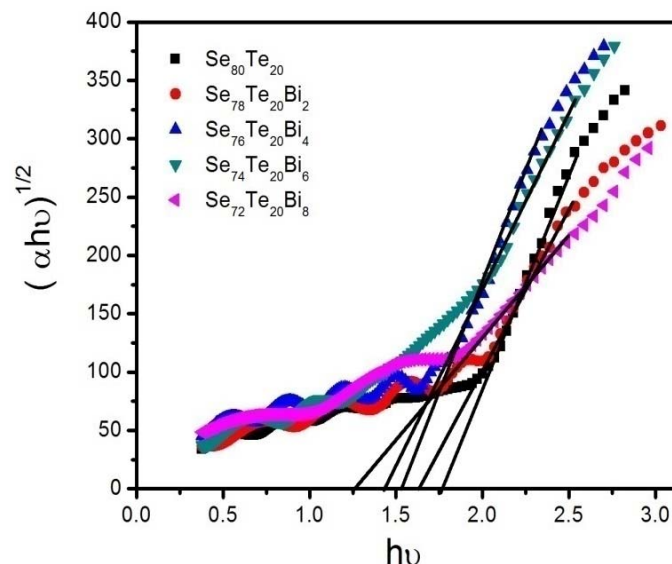


Fig 7. Variation of $(\alpha h\nu)^{1/2}$ with photon energy $(h\nu)$ for amorphous $Se_{80-x}Te_{20}Bi_x$ thin films.

These indirect band gap materials may have potential applications in optical recording media, infrared spectroscopy, laser fibers, xerography, fiber optic telecommunication and electrographic applications. Moreover, their refractive index and transparency in the infrared region are good indicators for integrated optics and detection in the near-infrared spectral domain.

4. Conclusion

Thin films of $Se_{80-x}Te_{20}Bi_x$ glassy alloys have been synthesized by thermal evaporation technique by using amorphous bulk alloy as a source material and glass as a substrate under high vacuum conditions ($\sim 10^{-4}$ Pa). The glassy nature of thin films has been checked with the help of X-ray diffraction technique. The optical transmission spectra of amorphous $Se_{80-x}Te_{20}Bi_x$ ($x = 0, 2, 4, 6, 8$) thin films have been measured by a double beam UV-VIS-NIR computer controlled spectrophotometer. Swanepole method has been used to calculate the refractive index, real and imaginary dielectric constant, extinction coefficient, absorption coefficient and optical band gap. The refractive index (n), extinction coefficient (k), real dielectric constant (ϵ'), imaginary dielectric constant (ϵ'') and absorption coefficient (α) increase with increase of photon energy. The optical band gap (E_g) decreases with increase of the Bi content. The decrease in optical band gap with increase of the Bi content may be due to increase in the density of defect states. The decrease in band gap could also be explained in terms of electronegativity difference between the elements. On the basis of above reported values of optical parameters, one may decide the suitability of these materials for device applications.

Reference

- [1] M. Sexsena, S. Gupta, A. Agarwal, Appl. Sci. Reseach **2(2)**, 109-116 (2011).
- [2] G. Kaur, T. Komastu, J. Mater. Sci. **36**, 453 (2001).
- [3] Z. Abdel-Khelek Ali, G. H. Adel, A. S. Abd-rao, Chalc. Lett. **6**, 125 (2009).

- [4] V. Trnovoca, I. Furar, D. Lezal, *J. Non-Cryst. Solids* **353**, 1311 (2007).
- [5] A. Kumar, P. B. Barman, R. Sharma, *adv. Apply. Sci. Research* **1(2)**, 47 (2010).
- [6] A. Kumar, M. Lal, K. Sharma, S. K. Tripathi, N. Goyal, *Ind. J. Pure and Appl. Phys.* **51**, 251 (2012).
- [7] A. Kumar, M. Lal, K. Sharma, S. K. Tripathi, N. Goyal, *chalc. Lett.* **9**, 275 (2012).
- [8] K. Sharma, M. Lal, A. Kumar, N. Goyal, *J. Non-Oxide Glasses* **6**, 1-11 (2014).
- [9] V. K. Sarawat, V. Kishore, K. Singh, N. S. Sexsena, T. P. Sharma, *Chalc. Lett.* **3**, 61 (2006).
- [10] R. M. Mehra, G. Kaur, P. C. Mathur, *J. Mater. Sci.* **26**, 3433 (1991).
- [11] A. B. Seddon, *J. Non-cryst. Solids* **44**, 184 (1995).
- [12] J. S. Sanghera, I. D. Agrwal, *J. Non-cryst. Solids* **6**, 256-257 (1999).
- [13] M. Saxena, *J. Physics D: Applied Physics* **38**, 460 (2005).
- [14] R. K. Shukla, S. Swaroup, A. Kumar, A. N. Nigam, *Phys. Stat. Sol. (a) K* **105**, 115 (1989).
- [15] H. Yang, W. Wang, S. Min, *J. Non-cryst. Solids* **80**, 503 (1986).
- [16] R. Chiba, N. Funakoshi, *J. Non-cryst. Solids* **105**, 149 (1988).
- [17] S. Shukla, S. Kumar, *Bull. Mater. Sci.* **34**, 1351–1355 (2011).
- [18] N. F. Mott, *Philos. Mag.* **19**, 835 (1969).
- [19] D.R. Macfarlane, M. Maecki, M. Paulain, *J. Non-Cryst. Solids* **64**, 351 (1984).
- [20] K. Matusita, T. Komatsu, R. Yokata, *J. Mater. Sci.* **19**, 291 (1984).
- [21] V.S. Shiryaev, J.L. Adam, X.H. Zhang, *J. Phys. Chem. Solids* **65**, 1737 (2004).
- [22] S. Mahadevan, A. Giridhar, A.K. Singh, *J. Non-Cryst. Solids* **88**, 11 (1986).
- [23] R. Swanepoel, *J. Phys. E.* **16**, 1214 (1983).
- [24] J. C. Manifacier, J. Gasiot, J. P. Fillard, *J. Phys. E. Sci. Instrum.* **9**, 1002 (1976).
- [25] S. M. Ei-Sayed, *Vaccum* **72**, 169 (2004).
- [26] H. S. Metcoally, *Vaccum* **62**, 345 (2001).
- [27] N. Suri, K.S. Bindra, M. Ahmad, J. Kumar, R. Thangaraj, *Applied Physics A, Materials and Processing* **90**, 149 (2008).
- [28] M. Ilyas, M. Zulfequar, M. Husain, *Optical Materials* **13**, 397 (2000).
- [29] Ambika, P. B. Barman, *J. Non-Oxide Glasses* **3**, 19-24 (2012).
- [30] N. F. Mott, E. A. Davis, *Electronic Processes in Non-Crystalline Mat.*, Clarendon, Oxford, 1979, 428.